

# COMBINED BLIND EQUALIZATION AND AUTOMATIC MODULATION CLASSIFICATION FOR COGNITIVE RADIOS UNDER MIMO ENVIRONMENT

Barathram Ramkumar (Wireless@VT, Bradley Department of Electrical and Computer Engineering, Virginia Tech, Blacksburg, VA-24060, bramkum@vt.edu );

Tamal Bose (Wireless@VT, Bradley Department of Electrical and Computer Engineering, Virginia Tech, Blacksburg, VA-24060, those@vt.edu);

Jeffrey H. Reed (Wireless@VT, Bradley Department of Electrical and Computer Engineering, Virginia Tech, Blacksburg, VA-24060, reedjh@vt.edu); and

Miloje S. Radenkovic (Electrical Engineering Department, University of Colorado, Denver, CO-80217, miloje.radenkovic@cudenver.edu).

## ABSTRACT

Blind equalization and Automatic Modulation Classification (AMC) have been of significant importance for cognitive radios when the receiver has no information about the channel or modulation type. Choosing an appropriate equalizer is difficult when the channel is Multi Input Multi Output (MIMO), and when there is no information about the channel. In this paper, an AMC based on cyclostationary feature detection and MIMO based Constant Modulus Algorithm (CMA) blind equalizers are used in conjunction. The probability of classification of the AMC is used as a metric and fed back to update the blind equalizer order. The equalizer and the AMC enhance the performance of each other. Computer simulations are given to illustrate the concept and yield promising results.

## 1. INTRODUCTION

One of the important aspects of cognitive radios is the ability to sense and characterize its RF environment and adapt accordingly [2]. Blind equalizers are used for recovering the transmitted input sequence using only the output signal with no knowledge of the channel. CMA is one of the popular blind equalization algorithms used for Single Input Single Output (SISO). The extension of CMA to MIMO systems is shown in [11]. It is also shown in [11] that the CMA equalizer can perfectly recover one of the input sequences from the output of the MIMO FIR channel thus reducing Co-Channel Interference (CCI) and Inter Symbol Interference (ISI).

Another important component of cognitive radio is AMC. AMC improves the spectral efficiency of cognitive radio by adapting transmission according to the spectral environment [1]. In this paper, cyclostationary based signal detection and pattern matching proposed in [6] and [7] are used. Neural

Networks trained using the Cyclic Domain Profiles (CDP) are used for signal classification due to their good pattern matching capabilities. It is shown in [6] that this AMC gives good performance under low SNR. The performance degradation of this AMC in the presence of the MIMO-FIR channel is shown.

When the channel information is not known, choosing the length of the equalizer becomes a difficult task. In this paper, a unified framework for MIMO cognitive radios is proposed, i.e. MIMO based CMA is used in conjunction with the AMC. The order of the blind equalizer is adjusted based on the probability of classification of the AMC.

This paper is organized as follows. In Section II, a brief background on blind MIMO equalization and MIMO based CMA is presented. In Section III, the spectral correlation based AMC is discussed. The proposed unified framework and the algorithm for adjusting the number of taps in the equalizer are discussed in Section IV. Simulation results are shown in Section V, followed by the conclusion in Section VI.

## 2. BLIND MIMO EQUALIZATION

The basic block diagram of the MIMO system is shown in Fig. 1. The  $d$  complex signals are passed through channels  $h_{ij}[n]$  for  $i=1\dots M$ , and  $j=1,\dots,d$  to generate  $M$  outputs ( $d < M$ ).

Let

$$x[n] = \begin{bmatrix} x_1[n] \\ \vdots \\ x_M[n] \end{bmatrix}, \quad a[n] = \begin{bmatrix} a_1[n] \\ \vdots \\ a_d[n] \end{bmatrix} \quad (1)$$

and

$$H[n] = \begin{bmatrix} h_{11}[n] & \cdots & h_{1d}[n] \\ \vdots & \vdots & \vdots \\ h_{M1}[n] & \cdots & h_{Md}[n] \end{bmatrix}. \quad (2)$$

The channel output  $x[n]$  is

$$x[n] = H[n] * a[n]. \quad (3)$$

Equation (3) can be written in the Z-domain as

$$x(z) = H(z)a(z), \quad (4)$$

where  $x(z)$ ,  $a(z)$  and  $H(z)$  are Z-transforms of  $x[n]$ ,  $a[n]$  and  $H[n]$  respectively.

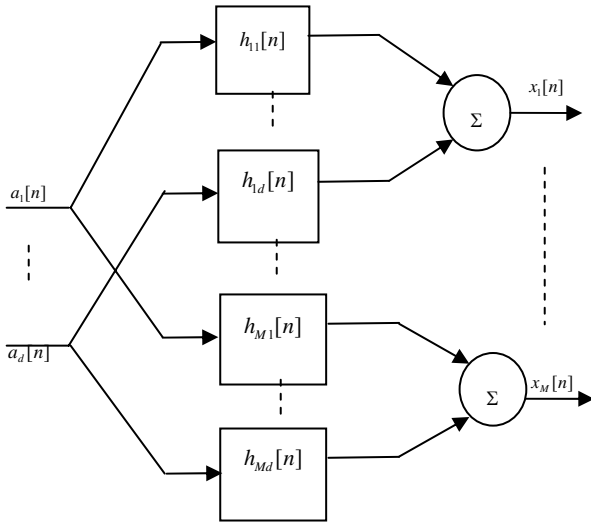


Fig1: MIMO-FIR Channel

Blind equalizers are used to recover the input sequence  $a[n]$  only from the output  $x[n]$ . The block diagram of the MIMO equalizer is shown in Fig.2. To recover the input sequence we need to find  $G[n]$  such that

$$G[n] * H[n] = I_d, \quad (5)$$

where  $I_d$  is a  $d \times d$  identity matrix and  $G[n]$  is the equalizer matrix given by

$$G[n] = \begin{bmatrix} g_{11}[n] & \cdots & g_{1M}[n] \\ \vdots & \vdots & \vdots \\ g_{d1}[n] & \cdots & g_{dM}[n] \end{bmatrix}. \quad (6)$$

Only the statistics of input signals are known, and hence the MIMO blind equalizer is subjected to phase and

permutation ambiguity. Therefore the best possible equalizer is

$$G(z)H(z) = PD(z), \quad (7)$$

where  $P$  is the permutation matrix and  $D(z)$  is the diagonal matrix defined as

$$D(z) = \text{diag}\{e^{j\theta_1} z^{-n_1}, \dots, e^{j\theta_d} z^{-n_d}\},$$

where  $\theta_i \in \{-\pi, \pi\}$ . The equalizer which satisfies (7) is known as the distortion-less recovery equalizer.

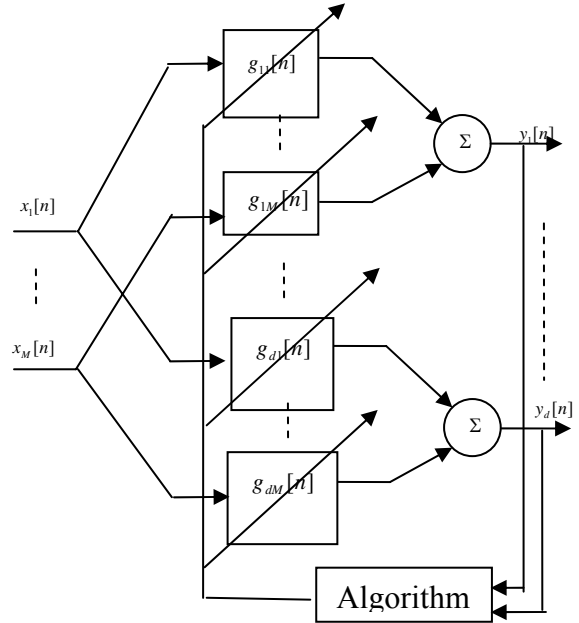


Fig 2: Blind Equalization for MIMO channels

### 2.1) CMA for MIMO FIR Channel

CMA for SISO is extended to MIMO systems in [11]. A brief overview of MIMO CMA from [11] is presented here. The block diagram of the MIMO CMA is shown in Fig 3. In order to recover the input sequence from the output  $x[n]$ , after each channel output, a linear filter is added. The coefficients of the filter are adjusted to minimize the Godard cost function [12], [13] and [14]:

$$C(y[n]) = \frac{1}{4} E\{(|y(n)|^2 - r)^2\}, \quad (8)$$

$$\text{where } r = \frac{m_4}{m_2},$$

and

$$m_2 = E\{|a_i[n]|^2\}, m_4 = E\{|a_i[n]|^4\}. \quad (9)$$

One of the important theorems from [11] is stated here.

*Theorem: For a MIMO FIR channel of length  $L$ , if  $H(z)$  is irreducible with  $H[L-1]$  being of full rank, then any MIMO-CMA FIR blind equalizer with length*

*$K \geq \left\lceil \frac{(L-1)d}{M-d} \right\rceil$  can achieve global convergence regardless of the initial setting.*

The above theorem states that the MIMO-CMA equalizer can recover one of the input signals, remove ISI, and suppress CCI, regardless of the initial setting.

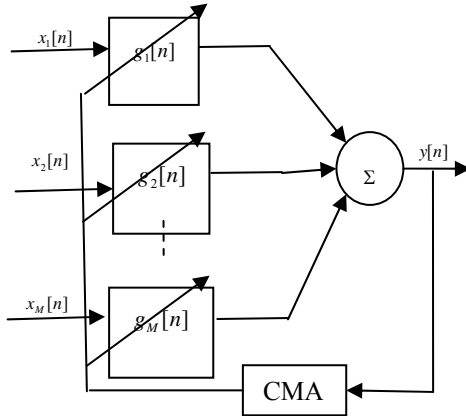


Fig 3: MIMO-CMA Blind Equalizer

### 3. CYCLOSTATIONARITY BASED AMC

#### 3.1. Background on cyclostationary spectral analysis.

If the mean and autocorrelation of a process  $x(t)$  is periodic, then the process is said to be a cyclostationary process [8] i.e.  $M_x(t+T_0) = M_x(t)$  and  $R_x(t+T_0, u+T_0) = R_x(t, u)$  for all  $t$  and  $u$ . Since the autocorrelation function is periodic it can be expressed as a Fourier series [9].

$$R_x(t + \frac{\tau}{2}, t - \frac{\tau}{2}) = \sum_{\alpha} R_x^{\alpha}(\tau) e^{j2\pi\alpha t}, \quad (11)$$

where

$$R_x^{\alpha}(\tau) = \lim_{Z \rightarrow \infty} \int_{-Z/2}^{Z/2} R_x(t + \frac{\tau}{2}, t - \frac{\tau}{2}) e^{-j2\pi\alpha t} dt. \quad (12)$$

The Wiener theorem for stationary processes can be extended to cyclostationary processes. The Spectral Correlation Function (SCF) is defined as a Fourier transform of (12)

$$S_x^{\alpha} = \int_{-\infty}^{\infty} R_x^{\alpha}(\tau) e^{-j2\pi f \tau} d\tau. \quad (13)$$

In practice there is only a limited number of samples available and hence SCF needs to be estimated from these samples. Let us define the cyclic periodogram as [10], [11]:

$$S_{xT}^{\alpha}(t, f) = \frac{1}{T} X_T(t, f + \frac{\alpha}{2}) X_T^*(t, f - \frac{\alpha}{2}), \quad (14)$$

where  $X_T(t, f)$  is the time invariant Fourier transform given by

$$X_T(t, f) = \int_{t-T/2}^{t+T/2} x(u) e^{-j2\pi f u} du. \quad (15)$$

The estimate of SCF can be obtained by the frequency smoothing of (14)

$$S_{xT}^{\alpha}(t, f)_{\Delta f} = \frac{1}{\Delta f} \int_{f-\Delta f/2}^{f+\Delta f/2} S_{xT}^{\alpha}(t, v) dv. \quad (16)$$

It is shown in [7] that SCF can be obtained by increasing the observation length  $T$  and decreasing  $\Delta f$ , that is

$$S_x^{\alpha}(f) = \lim_{\Delta f \rightarrow 0} \lim_{T \rightarrow \infty} S_{xT}^{\alpha}(t, f)_T. \quad (17)$$

#### 3.2. Spectral Coherence (SC) and $\alpha$ profile:

SCF is a correlation of frequency components shifted by  $f - \frac{\alpha}{2}$  and  $f + \frac{\alpha}{2}$ . It is intuitive to define Spectral Coherence (SC) as

$$C_x^{\alpha} = \frac{S_x^{\alpha}(f)}{[S(f + \frac{\alpha}{2})S(f - \frac{\alpha}{2})]^{\frac{1}{2}}}. \quad (18)$$

The magnitude of SC is always between 0 and 1. In order to reduce the computational complexity, one just uses the Cyclic Domain Profile (CDP) or  $\alpha$ -profile which is defined as

$$I(\alpha) = \max_f |C_x^{\alpha}(f)|. \quad (19)$$

#### 3.3. Automatic Modulation Classifier

Most modulated signals exhibit second order cyclostationarity [8]. From the CDP of the signal, important information about the signal like modulation type, keying rate, pulse shape, and carrier frequency can be obtained, [6] and [5]. Fig. 4 and Fig. 5 show the Cyclic Domain Profile (CDP) function for BPSK and QPSK respectively. To generate these plots the SQRC pulse with a roll off factor of 0.32 was used. Time domain and frequency domain smoothing were performed in order to estimate the SC. For time averaging the method suggested in [7] is used, i.e.

$$S_{xT}^{\alpha} = \frac{1}{N} \sum_{k=1}^N S_{xT}^{\alpha}(t_k, f). \quad (20)$$

$N= 20$  and  $T= 128$  are used, which means a total of  $N \times T = 1560$  samples were used.

The block diagram of the cyclostationarity based AMC is shown in Fig. 6. SCF creation and CDP extraction were discussed in the previous section. The final stage of the AMC is to classify the  $\alpha$ -profile using pattern matching. Pattern matching is performed using a feed forward neural network. The MAXNET structure shown in Fig. 7 is used. Each feed forward network has two hidden layers with 5 neurons in each layer, and the activation function used is  $\tanh(x)$ . The network is trained using the back propagation algorithm with an initial learning rate of  $\eta=0.05$  and a momentum constant of  $\alpha=0.7$ . The input to the feed forward network is the 200 point  $\alpha$ -profile and the output varies between  $[-1, 1]$ . The function of the MAXNET structure is to choose the highest value among all the feed forward networks.

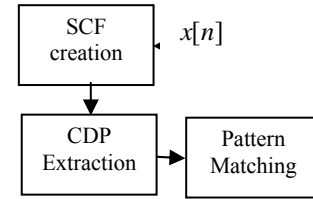


Fig 7: Block Diagram of the AMC.

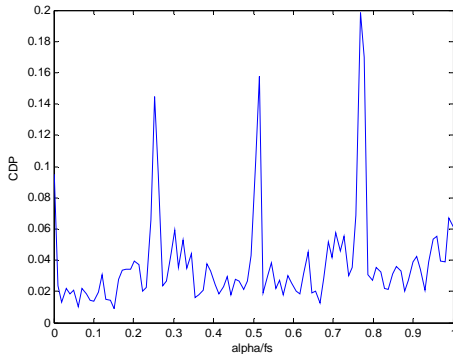


Fig 5: Cyclic Domain Profile for BPSK.

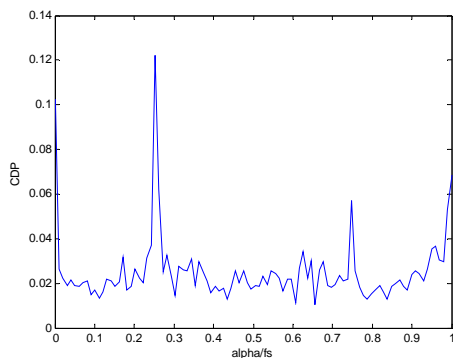


Fig 6: Cyclic Domain Profile for QPSK.

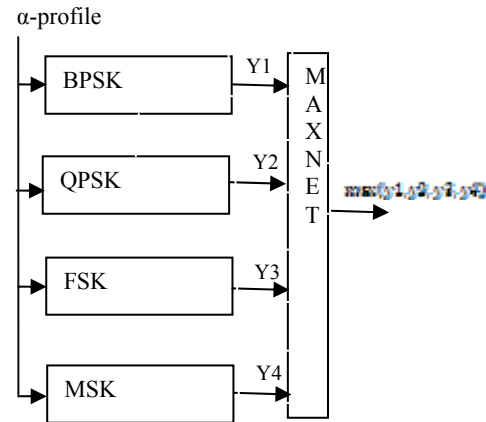


Fig 7: Neural Network structure.

#### 4. PROPOSED METHOD

In general, all fading channels are modeled as time varying FIR filters and hence the length of the above equalizer, i.e.  $K$ , plays an important role. When the receiver has no information about the channel, choosing the length of the equalizer ( $K$ ) is difficult. In this paper we choose the value of  $K$  based on the probability of classification of the AMC. The block diagram of the proposed method is shown in Fig 8. A simple algorithm to choose the value of  $K$  is shown below.

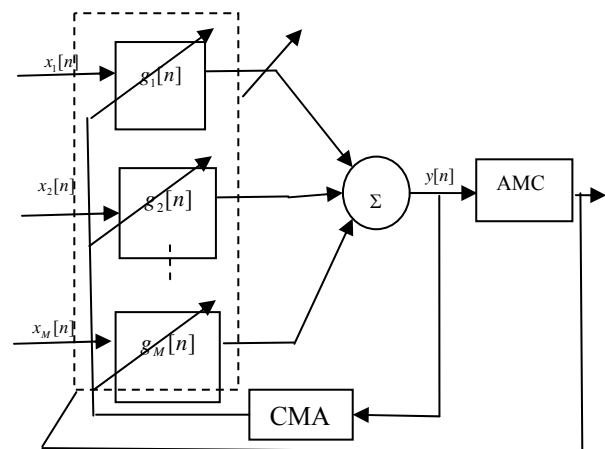


Fig 8: Proposed system block diagram

*Algorithm*

- Step 1: Choose a small initial length for the equalizer, i.e.  $K=2$ .
- Step 2: find the probability of classification for the AMC ( $p_a$ ).
- Step 3: increase the number of taps in the equalizer if  $p_a < p_{th}$ .
- Step 4: again find  $p_a$  and there is no need of updating if  $p_a > p_{th}$  or else repeat step 2.

**5. SIMULATION RESULTS**

*Experiment 1: To show the recovered symbol sequence and convergence.*

In this experiment a 2-input/3-output MIMO channel is considered, and the channel impulse response is given by

$$H[0] = \begin{bmatrix} -1.8 & -0.5 \\ -0.5 & 0.4 \\ -1.3 & 0.7 \end{bmatrix},$$

and

$$H[1] = \begin{bmatrix} 1 & -1.5 \\ -0.8 & 0.5 \\ 0.2 & -0.6 \end{bmatrix}.$$

Two QPSK sequences at SNR = 15dB is considered. The length of the equalizer considered was  $K=6$  and the learning rate considered was  $\mu = 0.0001$ . The received constellation of the signal before and after equalization is shown in Fig 9. It can be seen from the simulation that only one the sequence can be recovered, but we don't know which of the input signals. In order to show convergence, the cost function is plotted and number of iterations is shown in Fig 10.

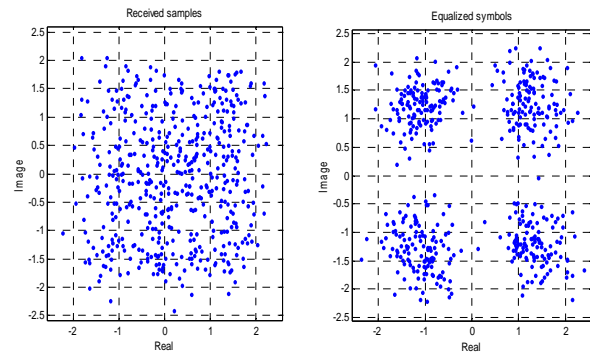


Fig 9: Received Samples  $x_1(n)$  and equalized symbols  $y(n)$ .

*Experiment 2: To show the performance of the AMC*

*a) Performance of AMC*

The network was trained with 500  $\alpha$ -profiles (each  $\alpha$ -profile has 200 points) of each BPSK, QPSK, FSK and MSK. No noise was added during the training process. The performance of the AMC in the presence of AWGN is evaluated using Monte Carlo simulations. Table 1 shows the probability of classification of AMC in the presence of the noise of SNR= 5dB. It is also shown in [7] that the performance of the AMC improves when the network is trained in the presence of noise of different variances.

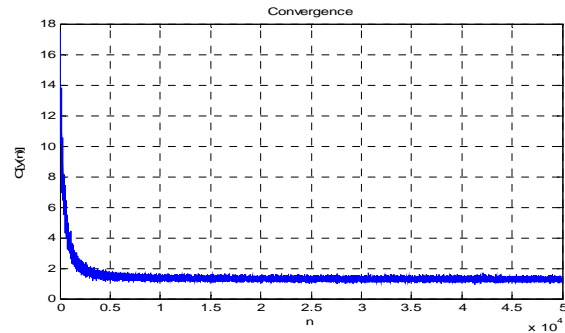


Fig 10: Convergence of CMA to one input sequence.

	<b>BPSK</b>	<b>QPSK</b>	<b>FSK</b>	<b>MSK</b>
<b>BPSK</b>	<b>0.999</b>	-	-	-
<b>QPSK</b>	-	<b>0.957</b>	-	<b>0.002</b>
<b>FSK</b>	-	<b>0.001</b>	<b>0.987</b>	-
<b>MSK</b>	-	-	-	<b>0.99</b>

Table 1: Probability of classification of AMC in the presence of AWGN (SNR = 5dB).

*b) Performance of AMC in the presence of a FIR channel.*

In this section, degradation in the performance of AMC due to the presence of the MIMO FIR channel is shown using simulations. The channel considered was a 2- input /3-output MIMO channel with each entry modeled as a random 8-Tap FIR filter. The 2-inputs considered were of the same modulation type and AMC was added to all 3-outputs. Monte Carlo simulation is performed on each output and the average probability of classification for each modulation scheme is presented in Table 2. The simulation results indicate that AMC provides inconsistent results in the presence of a multipath fading channel for a particular modulation scheme and hence the probability of correct classification decreases.

	<b>BPSK</b>	<b>QPSK</b>	<b>FSK</b>	<b>MSK</b>
<b>BPSK</b>	<b>0.41</b>	<b>0.20</b>	-	<b>0.39</b>
<b>QPSK</b>	<b>0.32</b>	<b>0.31</b>	-	<b>0.35</b>
<b>FSK</b>	-	<b>0.14</b>	<b>0.72</b>	<b>0.14</b>
<b>MSK</b>	<b>0.62</b>	-	-	<b>0.38</b>

Table 2: Probability of classification for AMC in presence of a MIMO FIR channel (SNR=5dB).

C) Performance of AMC in the presence of an equalizer of different lengths.

In this section the effect of using an equalizer of different order for a particular channel is shown using simulations. For the 2-input/3-output MIMO FIR channel considered in the previous section, MIMO CMA is added and one of the input sequences is recovered. The length of the MIMO CMA equalizer is varied. Monte Carlo simulations are performed and results are shown in Fig 11. The results show that the performance of AMC improves by increasing the order of the equalizer. These results illustrate the promise of the algorithm proposed.

5. CONCLUSION

In this paper, performance degradation of the cyclostationarity based AMC in the presence of a MIMO FIR channel was shown by simulation. MIMO CMA was implemented and it was shown that one of the input sequences can be recovered, suppressing the others. Hence by proper initialization, the desired signal can be obtained thereby reducing ISI and CCI. A combined MIMO CMA blind equalizer and AMC was proposed. The effect of the length of the equalizer on the performance of AMC was demonstrated based on a simple algorithm to update the length of the equalizer.

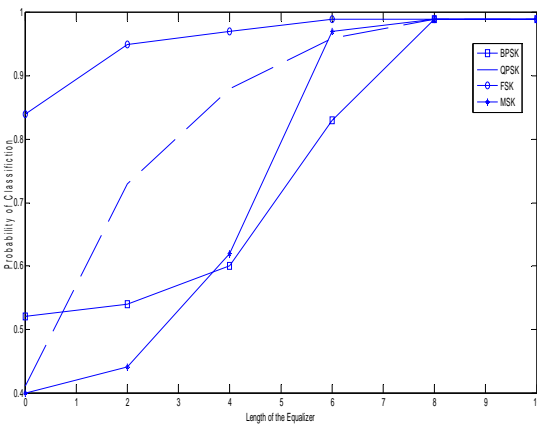


Fig 11: Effect of length of the equalizer on the performance of AMC (5dB noise).

6. REFERENCE

- [1] S. Haykin, "Cognitive radio: Brain-empowered wireless communications," IEEE J. Select. Areas Commun., vol. 23, pp. 201-220, 2005.
- [2] J. Polson, "Cognitive radio applications in software defined radio," in Proc. of the SDR Forum Conference, 2004.
- [3] S. Haykin, "Unsupervised adaptive filtering," Vol. II: Blind Deconvolution, John Wiley & Sons, Inc, 2000.
- [4] A. Fehske, J. Gaeddert and J. H. Reed, "A new approach to signal classification using spectral correlation and neural networks," in Proc. IEEE Dynamic Spectrum Access Nets, pp. 144-150, 2005.
- [5] K. Kim, I. A. Akbar, K. K. Bae, J. Um, C. M. Spooner, and J. H. Reed, "Cyclostationary approaches to signal detection and classification in cognitive radios," in Proc. IEEE Dynamic Spectrum Access Nets., pp. 212-215, 2007.
- [6] W. A. Gardner, Introduction to Random Process with Applications to Signals and Systems. MacMillan, 1986.
- [7] W. A. Gardner, Statistical Spectral Analysis A Nonprobabilistic Theory. Prentice Hall, 1988.
- [8] R. S. Roberts, "Computationally efficient algorithms for cyclic spectral analysis," IEEE Signal Processing Mag, Apr. 1991.
- [9] W. M. Gardner, "Measurement of spectral correlation," IEEE Trans on Acoust, Speech, and Signal Processing, Vol. ASSP-34, no. 5, Oct.1986
- [10] W. M. Gardner and C. M. Spooner, "Signal interception: Performance advantages of cycle-feature detectors," IEEE Trans Commun, vol. 40, no.1, Jan. 1992.
- [11] Y. Li, and K. J. Ray Liu, "On Blind Equalization of MIMO Channels", IEEE International Conference on Communication, vol. 2, pp.1000-1004, 1996.
- [12] D. N. Godard, "Self-recovering equalization and carrier tracking in two-dimensional data communication systems," IEEE Trans. Commun., COM-28:pp. 1867-1875, 1980.
- [13] J. R. Treichler and M.G. Larimore, "New processing techniques based on the constant modulus adaptive algorithm," IEEE Trans. Acoust, Speech Signal Processing, ASSP-33, pp. 420-431, 1985.
- [14] J. R. Treichler and B. G. Agee "A new approach to multipath correction of constant modulus signals," IEEE Trans. Acoust, Speech Signal Processing, ASSP-31, pp. 349-372, 1983.

